Available online at www.sciencedirect.com
SCIENCE DIRECT®
C. R. Physique 7 (2006) 56–67
COMPTES RENDUS PHYSIQUE
http://france.elsevier.com/direct/COMREN/

Superconductivity and magnetism/Supraconductivité et magnétisme

Magnetism and superconductivity in rare earth–nickel–borocarbides

Sergey L. Bud'ko *, Paul C. Canfield

Ames Laboratory US DOE and Department of Physics and Astronomy, Iowa State University, Ames, IA 50011, USA

Available online 19 January 2006

Abstract

The $R\mathrm{Ni_2B_2C}$ (R = Gd–Lu, Y) series of compounds offers a spacious testing ground for the interaction between $4f$ and conduction electrons and specifically for interactions between local magnetic moments and the superconducting ground state. In this review we will survey the effects that local moments have on the superconducting transition temperature (T_c), the upper superconducting critical field ($H_{c2}(T)$) and the vortex pinning and critical current density (J_c). ***To cite this article: S.L. Bud'ko, P.C. Canfield, C. R. Physique 7 (2006).***

Résumé

Magnétisme et supraconductivité dans les borocarbures de terres rares et de nickel. La série des composés $R\mathrm{Ni_2B_2C}$ (R = Gd–Lu, Y) offre un vaste champ d'investigation pour tester l'interaction entre les électrons 4f et les électrons de conduction et, plus spécifiquement, les interactions entre les moments magnétiques localisés et l'état fondamental supraconducteur. Dans cette revue, nous étudierons les effets des moments localisés sur la température de transition supraconductrice (T_c), sur le second champ critique ($H_{c2}(T)$), ainsi que sur l'ancrage des vortex et la densité de courant critique (J_c). ***Pour citer cet article : S.L. Bud'ko, P.C. Canfield, C. R. Physique 7 (2006).***

Keywords: $R\mathrm{Ni_2B_2C}$; Superconductivity; Magnetism

Mots-clés : $R\mathrm{Ni_2B_2C}$; Supraconducteur ; Magnétisme

1. Introduction

The $R\mathrm{Ni_2B_2C}$ ($R1221$) series of magnetic superconductors was discovered in 1994 [1] and, over the past decade has become one of the best characterized families of magnetic superconductors ever studied. This is partly due to the wide range of temperatures over which both magnetism and superconductivity co-exist (see Fig. 1 for plot of T_c and T_N for pure compounds as a function of the de Gennes (dG) factor), partly due to the early, ready availability of high purity single crystal samples, and partly due to the revolution in automated data collection for temperature and field dependent thermodynamic and transport measurements that started taking place in the late 1980s. The $R\mathrm{Ni_2B_2C}$ family was discovered as a result of the report of curiously high temperature superconductivity thought to exist in Y–Ni–B system [2]. This report spurred research that lead to the nearly simultaneous publication of reports of superconductiv-

* Corresponding author.
E-mail address: budko@ameslab.gov (S.L. Bud'ko).

1631-0705/$ – see front matter
doi:10.1016/j.crhy.2005.11.011

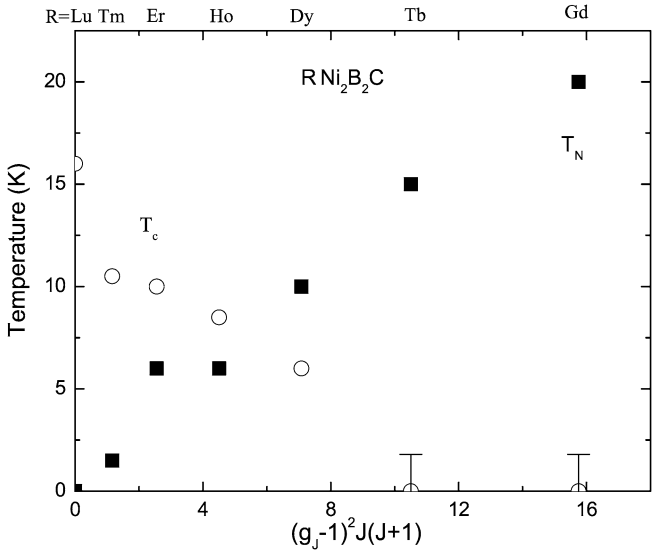

Fig. 1. T_c and T_N versus the de Gennes factor for pure $R\mathrm{Ni}_2\mathrm{B}_2\mathrm{C}$ compounds.

ity in a Y–Ni–B–C quaternary compound [3] that was identified to be a filled variant of the $\mathrm{ThCr}_2\mathrm{Si}_2$ structure with stoichiometry $\mathrm{YNi}_2\mathrm{B}_2\mathrm{C}$ [1] and with a T_c of ≈16 K. $\mathrm{YNi}_2\mathrm{B}_2\mathrm{C}$ is just one of the members of the $R\mathrm{Ni}_2\mathrm{B}_2\mathrm{C}$ family that superconducts. Superconductivity was originally reported for $R = \mathrm{Y}$, Lu, Tm, Er, and Ho and was later discovered for $\mathrm{DyNi}_2\mathrm{B}_2\mathrm{C}$ as well, [4]. In addition Cava and co-workers also discovered a metastable Pd-based version of this structure [5] with stoichiometry $\mathrm{YPd}_2\mathrm{B}_2\mathrm{C}$, with $T_c \approx 23$ K that, at the time, rivaled the highest intermetallic T_c-value found for $\mathrm{Nb}_3\mathrm{Sn}$.

Whereas the initial research emphasis on the $R\mathrm{Ni}_2\mathrm{B}_2\mathrm{C}$ family was on the coexistence and interplay between the rare earth, local moment, magnetism and superconductivity, as more and more work was performed on the family it was found that the $R\mathrm{Ni}_2\mathrm{B}_2\mathrm{C}$ series held a plethora of model systems that encompassed many of the themes in modern correlated electron and superconductivity research: non-locality and flux line lattice transitions, heavy fermion physics, phonon softening/proximity to structural phase transitions, and complex, yet comprehensible metamagnetism [6–8]. The $R\mathrm{Ni}_2\mathrm{B}_2\mathrm{C}$ series turned out to be a toy-box for the solid state physicist. In this article we will review the interaction between superconductivity and magnetism in this series. Even this subset of $R\mathrm{Ni}_2\mathrm{B}_2\mathrm{C}$ research is a huge field with hundreds of research papers published on it. With this in mind, for this review we will refer primarily to work that has been performed on single crystalline samples, primarily from the Ames Laboratory.

2. Non-magnetic superconductors: pure and doped

Before examining the physics associated with the interaction between a Bravais lattice of local moments and a superfluid, it is important to first understand a little about the non-magnetic members of the series (Lu1221 and Y1221) and how they respond to minor perturbations. This can be done via substitutions on the rare earth site (magnetic perturbations) or via substitutions on the non-moment-bearing Ni site (non-magnetic perturbations).

Lu1221 and Y1221 have relatively high T_c values (∼16.2 K and ∼15.6 K respectively) and can be synthesized so as to have very low, normal state, residual resistivities (≈1 μΩ cm). As a result, both of these materials are near the clean limit with $l > \xi_0$. This allows for the observation of non-local effects, the most dramatic of which is the field driven, structural phase transition in the flux line lattice from a low field, hexagonal arrangement to a higher field square arrangement at an applied field, H_2. Once this effect was discovered (originally in Er1221 [9] and then later in Y1221 [10] and Lu1221 [11–13]) (see Fig. 2 for an example) an elegantly simple theoretical explanation was devised [14]. One of the particularly appealing aspects of this theory was its predictive power, i.e., that the critical field associated with the transition would be a simple function of ξ_0/l. (At the simplest level this can be understood by the fact that for non-local effects, the electrons should not scatter too much as they flow around the core of the vortex as part of the screening current.) In order to test this theory and its predictions, a series of $\mathrm{Lu}(\mathrm{Ni}_{1-x}\mathrm{Co}_x)_2\mathrm{B}_2\mathrm{C}$ samples were grown

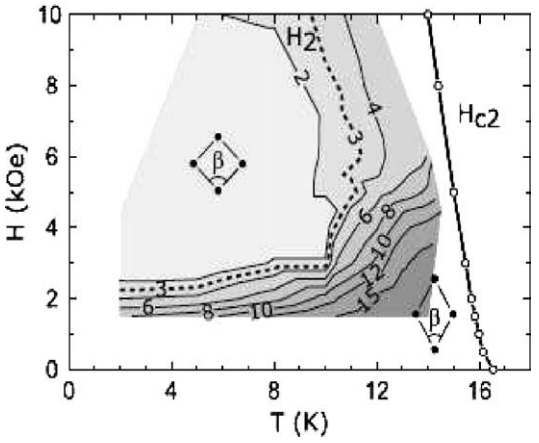

Fig. 2. Schematic H–T flux line lattice phase diagram for $LuNi_2B_2C$ ($H \| c$). See [13] for a detailed discussion.

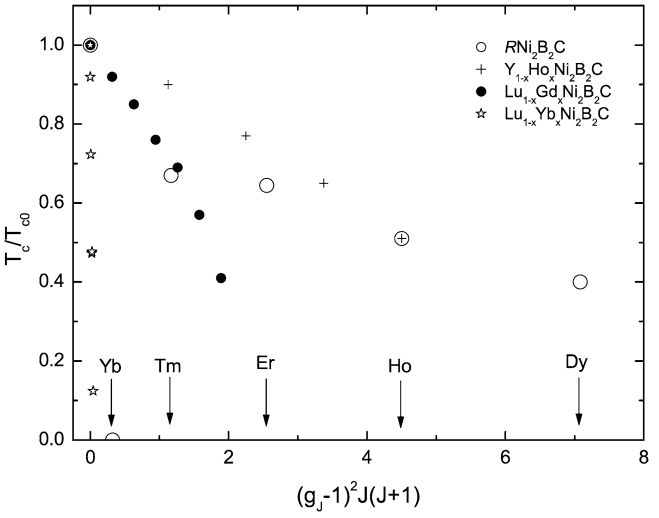

Fig. 3. T_c versus the de Gennes factor for pure $R Ni_2B_2C$ compounds and several series of solid solutions.

and measured. As Co was titrated onto the Ni site, the residual resistivity monotonically increases, implying that the electronic mean free path, l, monotonically decreases, and the ratio of ξ_0/l increases [15]. These and other results are displayed in Table 1. The theory by Kogan et al. [16–18] predicts an increase in the critical field needed to stabilize the square FLL, and indeed the measured values of H_2 agree with the theoretical predictions [14].

Table 1 indicates that the non-local London theory describes the physics of these systems quite well; it also points out that whatever the nature of the superconductivity in $LuNi_2B_2C$, it is not very sensitive to the ratio of ξ_0/l. At a minimum this rules out some of the more fragile, exotic gap symmetries such as those associated with Sr_2RuO_4 [19]. On this note though, it is worth noting that the nature of the superconducting gap symmetry associated with the $R Ni_2B_2C$ materials is still open to debate. A variety of measurements indicated that there must be substantial gap anisotropy, but whether the gap actually has nodes in it or not is still an open question.

A much more common form of perturbation, particularly for magnetic superconductors, is the magnetic impurity. For the case of the $R Ni_2B_2C$ family $R =$ Gd–Yb can be added. Fig. 3 shows the effects of representative magnetic impurities on the T_c of $LuNi_2B_2C$ and YNi_2B_2C. As can be seen, T_c is suppressed to varying degrees by different impurities. For example, even a 100% substitution of Tm for Lu only suppressed T_c from 17 to 12 K. On the other hand as little as 20% Gd or 13% Yb suppressed T_c to $\leqslant 2$ K. If we were to expect a simple de Gennes scaling of the suppression of T_c, then the manifold defined by $(Lu_{1-x}Gd_x)Ni_2B_2C$ data should be the locus of all of the T_c(dG) data points. As can be seen, this is not the case. Whereas the T_c for Tm1221 does coincide with the $(Lu_{1-x}Gd_x)Ni_2B_2C$ manifold, the data for the other local moments impurities appears to manifest much higher T_c values than would be predicted for their dG factor. This deviation from simple dG scaling of T_c has been associated with the highly anisotropic nature (essentially planar for $T < 20$ K) of the local moments for $R =$ Er–Tb. The effect of this anisotropy can be understood, in simply terms, as a reduction of the phase space available for Cooper pair breaking due to spin-

Table 1
Experimental values of T_c, ρ_0, $\rho(300\text{ K})/\rho_0$ and $H_{c2}(0)$ from resistivity measurements and estimated values of l, ξ_0, ξ_0/l, and H_2 for $Lu(Ni_{1-x}Co_x)_2B_2C$ (after [15])

Nominal x	T_c (K)	ρ_0 (μΩ cm)	$\rho(300\text{ K})/\rho_0$	$H_{c2}(0)$ (kOe)	l (Å)	ξ_0 (Å)	ξ_0/l	H_2 (kOe)
0	16.0	1.5	24.0		270	310	1.1	0.8
0.015	14.9	4.2	9.4	60	100	330	3.3	3.4
0.03	14.2	5.7	7.4	55	70	350	5	4.9
0.045	12.9	8.1	5.5	43	50	390	7.8	10.5
0.06	11.4	11.6	4.1	33	40	440	11	15.3
0.09	9.5	14.5	3.5	22	30	520	17	25.4

flip scattering in the paramagnetic state, i.e., if the low temperature state of the local moments were not so anisotropic, then the T_c(dG) data point would be on the $(Lu_{1-x}Gd_x)Ni_2B_2C$ data manifold.

The most aggressive pair breaking impurity though is not Gd, but Yb instead [20]. This is due to the fact that $YbNi_2B_2C$ is a model Yb-based heavy fermion compound with the Yb ions strongly hybridizing with the conduction electrons near and below a characteristic temperature, $T_K \sim 10$ K [21,22]. At the crudest level this can be put into a dG scaling context by realizing that for conventional de Gennes scaling the interaction between the local moment and the conduction electrons is assumed to be constant across the rare earth series. For the case of a hybridizing ion such as Yb this assumption is clearly invalid and the interaction between the $4f$ electrons and conduction electrons can be much larger. A more complete treatment of the suppression of superconductivity by hybridizing local moments reveals that the suppression of T_c is most aggressive when $T_c \leqslant T_K$ [23–25]. This is close to the case for Yb ions ($T_K \sim 10$ K for pure Yb1221) in Lu1221 ($T_c \sim 16$ K).

We can already see that the interaction between the local moments associated with the rare earths and the superconductivity associated with the conduction electrons will be a rich phase space for exploration. Whereas there are some nuances associated with the effects that impurities have on the superconducting states of Lu1221 and Y1221, they can apparently be integrated into our general understanding how impurities effect superconductivity. On the other hand the R1221 series offers us the opportunity to see what happens when we actually have an ordered lattice of local moments interacting with the superconducting electrons.

3. Magnetic superconductors and superconducting antiferromagnets

One of the beauties of the RNi_2B_2C family of magnetic superconductors is the fact that a wide variety of rare earths can be substituted on the R site, and in virtually arbitrary proportions. This allows for the study of T_c and T_N as a function of the concentration and type of rare earth used. As can be seen in Fig. 3 for (Y/Ho)1221, T_c progresses in a near linear manner between the T_c for pure Y1221 (∼15 K) and the T_c for pure Ho1221 (∼8 K). In a similar manner the T_c for, e.g., (Y/Er)1221 [26] progresses in a near linear manner between ∼15 and ∼10.5 K.

This rather trivial behavior disappears when a series of samples between Ho1221 and Dy1221 is examined [27]. As can be seen in Fig. 1, for R = Tm, Er, and Ho members of the R1221 series $T_c > T_N$. On the other hand, for Dy1221 $T_N > T_c$. This means that somewhere between Ho1221 and Dy1221 the T_c and T_N phase lines must cross. Fig. 4 presents T_c and T_N data for the $(Ho_{1-x}Dy_x)Ni_2B_2C$ series. Although the T_N rises from Ho1221 to Dy1221 in a monotonic, linear manner, T_c versus dG is very non-linear. As can be seen, T_c does drop until near 30% Dy, the concentration at which $T_c \approx T_N$. From that point onward, T_c is essentially independent of Dy concentration (and therefore dG factor). In order to more fully understand this behavior, Fig. 5 presents transition temperature versus

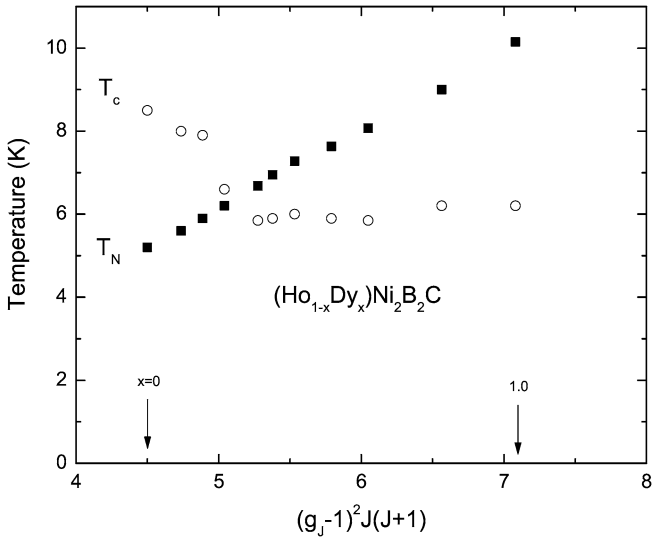

Fig. 4. T_c and T_N versus the de Gennes factor for $(Ho_{1-x}Dy_x)Ni_2B_2C$ (after [27]).

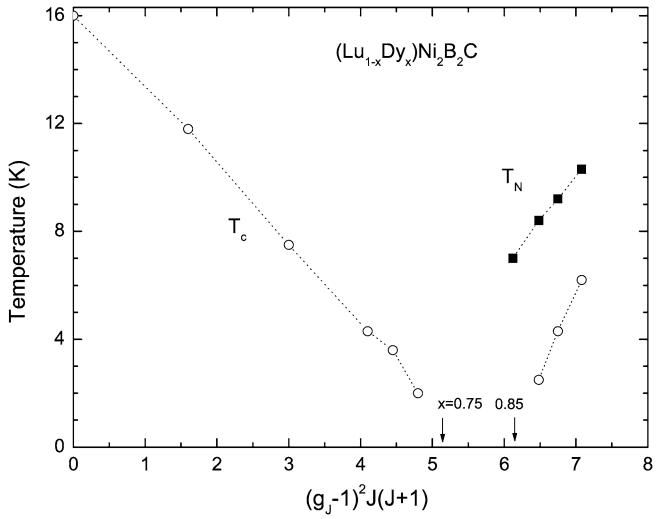

Fig. 5. T_c and T_N versus the de Gennes factor for $(Lu_{1-x}Dy_x)Ni_2B_2C$ (after [27]).

dG factor for a (Lu/Dy)1221 series [27]. In this case an even more remarkable result presents itself: T_c is not only suppressed when Dy is added to Lu1221, but T_c is also suppressed when Lu is added to Dy1221. The combination of the (Lu/Dy)1221 and (Ho/Dy)1221 data sets helped to reveal that Dy1221 was indeed a very novel example of coexistence between magnetism and superconductivity: a superconducting antiferromagnet, i.e., a compound that only superconducts because the antiferromagnetic state reduces the spin-flip scattering by the Dy ions. This can be understood by recalling what give rise to the pairbreaking associated with dilute magnetic impurities in a non-magnetic host: spin-flip scattering; a Cooper pair is broken when one of the electrons reverses it sign due to a spin-flipping interaction with an isolated impurity. In the case of (Lu/Ho)1221 this scattering is weak enough that even for pure Ho1221 there is a finite T_c in the paramagnetic state. On the other hand, the data from the (Lu/Dy)1221 series indicates that the spin flip scattering from the Dy ions is so strong that paramagnetic Dy1221 cannot support superconductivity.

On the other hand, $DyNi_2B_2C$ does superconduct. This superconductivity occurs because the Dy ions order antiferromagnetically and pair breaking by flipping the spin of a single Dy ion is no longer a possibility; instead for pairbreaking taking place, there needs to be an interaction between a Cooper pair and a magnon, a magnetic excitation. This observation allows for the explanation of the Dy-rich sides of both the (Lu/Dy)1221 and (Ho/Dy)1221 plots. In the case of (Lu/Dy)1221 as Lu is substituted for Dy there is a strong suppression of T_N and a dramatic increase in the magnetic disorder and the magnetic disorder scattering. This is not surprising since Lu is non-magnetic and acts as a huge perturbation to the magnetic sublattice. This softening of the magnetically ordered state leads to a dramatic increase in pair breaking and T_c is rapidly suppressed. On the other hand as Ho is substituted for Dy there is very little perturbation to the magnetic sublattice and very little change in either the thermodynamic or transport properties. Ho has a similar local moment size as well as anisotropy. As Ho is titrated in for Dy there is very little change in either the magnetic disorder or the magnetic disorder scattering and as a result, T_c remains essentially unchanged. These data indicate that superconductivity in Dy1221 is the result of a very delicate balance and will be very sensitive to any perturbations to the long range order in Dy1221.

4. Magnetic field–temperature phase diagrams: effects on $H_{c2}(T)$

The interplay between local moment magnetism and superconductivity manifests itself even more clearly in an applied magnetic field. To this end the study of H–T phase diagrams (both for the superconducting and ordered local moment phases) is enlightening.

The local moment anisotropy of the Tm^{3+} ion is moderately axial and the local moment anisotropy of the Er^{3+}, Ho^{3+} and Dy^{3+} ions is extremely planar. Fig. 6 shows the temperature-dependent, anisotropic magnetic susceptibility for Tm1221 as well as that for Er1221 [28,29]. This anisotropy, associated with the paramagnetic state, gives rise to a corresponding anisotropy in $H_{c2}(T)$ (see Fig. 7). The anisotropy in $H_{c2}(T)$ found for Tm1221 and Er1221 (Fig. 7(a))

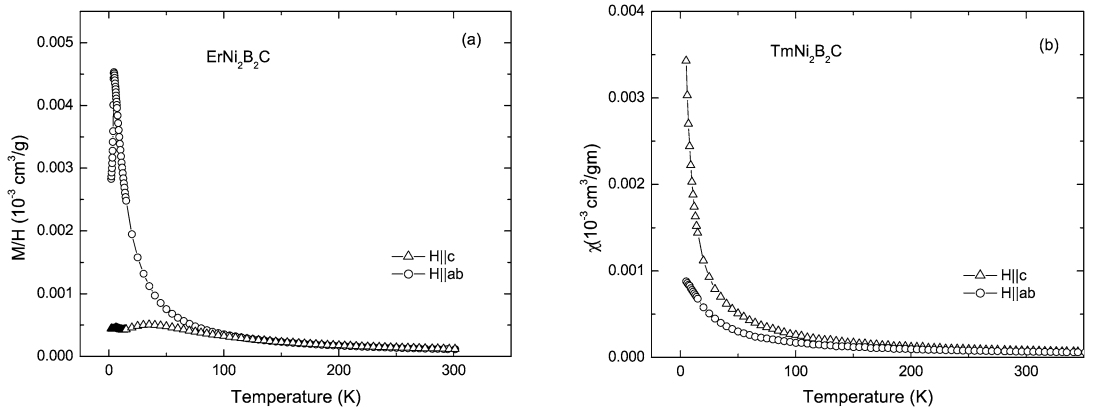

Fig. 6. (a) Anisotropic temperature-dependent susceptibility for (a) Er1221 [28], and (b) Tm1221 [29].

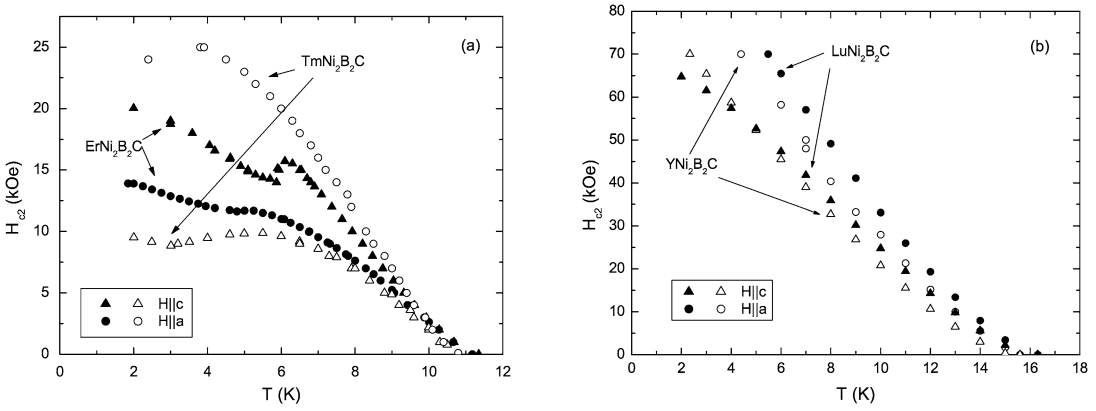

Fig. 7. (a) Anisotropic $H_{c2}(T)$ for Tm1221 (open symbols) and Er1221 (filled symbols) for $H\|[001]$ (triangles) and $H\|[100]$ (circles); (b) anisotropic $H_{c2}(T)$ for Y1221 (open symbols) and Lu1221 (filled symbols) for $H\|[001]$ (triangles) and $H\|[100]$ (circles).

is much more substantial than that found for the non-magnetic Y1221 or Lu1221 [30] (see Fig. 7(b)) and, more importantly, the sign of this anisotropy can be associated with the changed local moment anisotropy. For Tm1221 the $H_{c2}(T)$ curve for $H \parallel c$ is lower than that for $H \perp c$ because for $H \parallel c$ there is a substantially larger sublattice magnetization contributing to the internal field that is suppressing the superconducting ground state. For Er1221 the $H_{c2}(T)$ for $H \parallel c$ is larger than that for $H \perp c$ for exactly the same reason: for $H \perp c$ the Er1221 susceptibility is substantially larger than for $H \parallel c$.

The form of $H_{c2}(T)$ is also dramatically effected by the anisotropy and the state of the local moment sublattice [31–33]. For Tm1221 $H_{c2}(T)$ goes through a broad, local maximum that has been associated with the competition between a growing sublattice susceptibility (as temperature is decreased) and a less rapidly increasing 'bare' H_{c2}, associated with the superconducting electrons in the absence of the paramagnetic Tm ions. For temperatures below this maximum, $H_{c2}(T)$ decreases with decreasing temperature because the internal field associated with the sublattice magnetization is growing more rapidly than the 'bare' H_{c2} term.

A more dramatic example of how the form of $H_{c2}(T)$ is effected by the local moment sublattice can be seen in data on Er1221 and Ho1221 (Figs. 8 and 9). Er1221 orders antiferromagnetically at ∼6 K with a wave vector of ∼0.55 a^*, a vector that has been associated with a local maximum in the generalized electronic susceptibility and with phonon softening in the non-magnetic Lu1221 and Y1221, i.e., a wave vector associated with some degree of Fermi-surface nesting [34]. The Er1221 $H_{c2}(T)$ data for $H \parallel c$ shows a very sharp drop in H_{c2} at the point where, in the H–T phase diagram $H_{c2}(T)$ crosses from the paramagnetic, higher temperature state to the antiferromagnetically ordered, lower temperature state (Fig. 8). Just such a drop was predicted for the case of an antiferromagnetic superconductor which has an ordering wave vector determined by a maximum in $\chi(q)$ [35,36]. In order to further investigate this

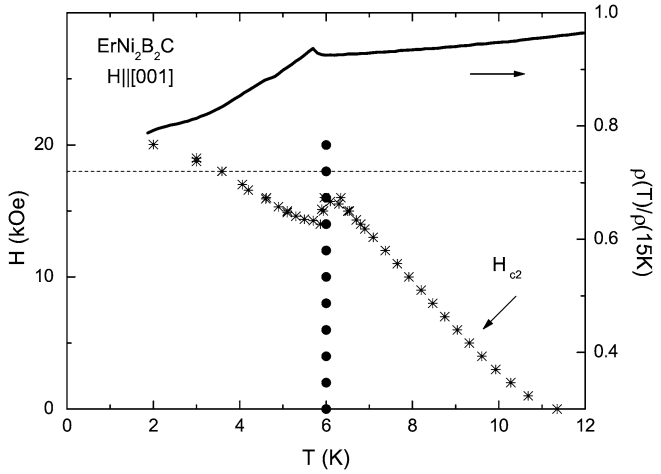

Fig. 8. Composite H–T phase diagrams for Er1221 ($H\|[001]$ with overlayed resistivity data. Symbols: $*$—H_{c2}, •—T_N. Dotted line show where resistivity data (shown in the upper part of the panel) were taken (after [34]).

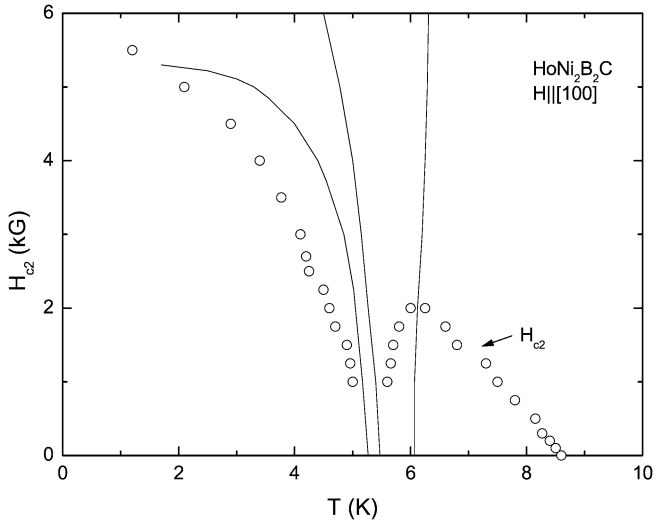

Fig. 9. Example of composite H–T phase diagram for Ho1221 ($H\|[100]$). Lines—magnetic phase boundaries, circles—$H_{c2}(T)$ (after [39]).

phenomenon, electrical resistivity was measured as a function of temperature for $H\|c$ just slightly greater than 10 kOe for the current flowing along the [100] direction. As can be seen these data manifest an increase in resistivity at T_N that can be associated with a superzone gap (Fig. 8). These data all support the conclusion that the sharp drop in $H_{c2}(T)$ at T_N is associated with the local moment state ordering with an 0.55 a^* wave vector.

This phenomenon can be probed even further by examining the $H_{c2}(T)$ data for Ho1221 and plotting it on top of the magnetic H–T phase diagram. In the case of Ho1221 the magnetic order is quite complex: the 0.55 a^* phase only exists over a very limited temperature range; between ∼6 and ∼5 K (Fig. 10) [37,38]. Below ∼5 K the magnetic order has a [001] wave vector. The effects of this can be seen in the composite (magnetic and superconducting) H–T phase diagram (Fig. 9) [39]. Initially, just below T_c, $H_{c2}(T)$ rises. On cooling through $T_N \approx 6$ K the 0.55 a^* phase starts to grow and $H_{c2}(T)$ decreases. On cooling through ∼5 K the 0.55 a^* order is replaced by a commensurate antiferromagnetic order and $H_{c2}(T)$ recovers dramatically.

The Er1221 and Ho1221 data taken together quite clearly indicate that the dip in $H_{c2}(T)$ is related to ∼0.55 a^* phase, which itself is related to a maximum in the generalized electronic susceptibility. It is worth noting that whereas the local minimum in the $H_{c2}(T)$ of Ho1221 appears to be much deeper than that seen for Er1221, the size of the drop in $H_{c2}(T)$ in absolute units (kOe) is essentially the same.

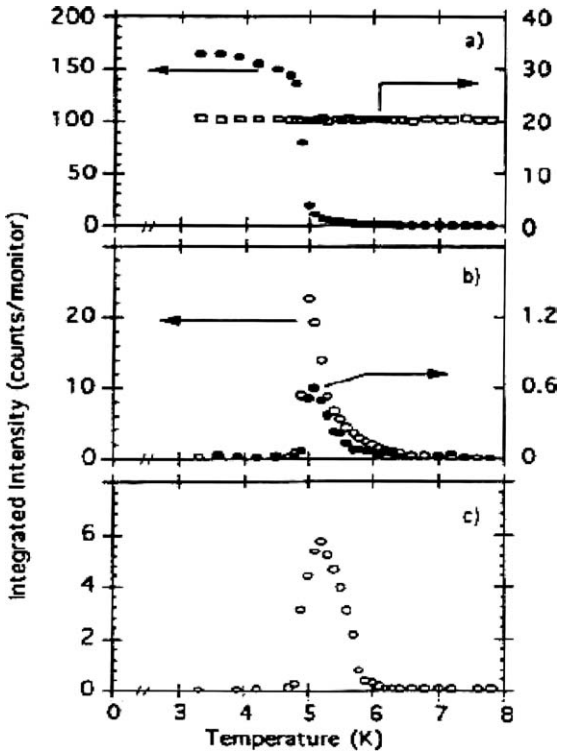

Fig. 10. Temperature dependence of (a) the (003) commensurate AFM peak (•) and the (101) nuclear Bragg peak (□); (b) the first- (○) and third-order (•) satellites associated with the modulation wave-vector, $K_1 = 0.915\ c^*$; and (c) the $K_2 = 0.585\ a^*$ magnetic satellite (after [37]).

To complete the discussion of the effects of ordering on $H_{c2}(T)$ we can recall that for Dy1221 the local moment ordering is the same as that seen in the low temperature phase of Ho1221, and as we discussed earlier, the superconducting state in pure Dy1221 only exists as a result of this ordering. For Ho1221 $H_{c2}(T)$ recovers in the 1.0 c^* ordered state. In the case of Dy1221 T_c (and implicitly $H_{c2}(T)$) only exist below this ordering temperature.

5. Coexistence of superconductivity and weak ferromagnetism

The coexistence of superconductivity with antiferromagnetic order is not too surprising for compounds that have superconducting coherence lengths much larger than the magnetic unit cell dimension (in practice this is almost always the case). On the other hand the coexistence of superconductivity with ferromagnetism is a very rare and exotic thing given that these two ground states are highly antagonistic. This can be readily seen in $ErRh_4B_4$ which superconducts with a T_c of 8.7 K and then re-enters the normal state just 0.1 K below the onset of ferromagnetic order at $T_C = 0.9$ K [40–42]. Detailed experimental and theoretical studies of the magnetic ordering wave vector showed that initially the magnetic and superconducting ground states attempt a compromise ground state where superconductivity coexists with the magnetic state being a combination of a ferromagnetic structure and a transversely linearly polarized modulated structure with a wavelength of ∼100 Å [41,42]. Ultimately the free energy gain associated with ordering the local moments so greatly exceeds the free energy gain associated with the superconducting ground state the superconducting state can no longer exist and the sample enters a normal, ferromagnetic, low-temperature state. Once this was understood it was suggested that if a much more dilute ferromagnetic system could be synthesized it was possible that coexistence between ferromagnetism and superconductivity, with exotic consequences such as spontaneous vortex states, may actually be realized. Unfortunately such compounds were not readily discovered.

$ErNi_2B_2C$ has a superconducting T_c of ∼11 K and an antiferromagnetic T_N of ∼6 K, but below $T_{WF} \sim 2.3$ K the magnetic ordering of Er1221 acquires a ferromagnetic component: $\sim 0.33\ \mu_B$/Er at $T = 2.0$ K [43] (this can be compared to the full saturated moment of 9.0 μ_B/Er). This ordering is associated with a locking of the incommensurate ordering wave vector into a value of ∼0.55 a^* and a squaring of the order associated with the extreme local moment

anisotropy. Such order leads to a greatly reduced, net saturated moment and an equally reduced estimate of the equivalent, internal field associated with this small ferromagnetic component; comparable to H_{c1} and much smaller than H_c and very much smaller than H_{c2}. The existence of this ferromagnetic component, first inferred from thermodynamic measurements, has been confirmed by a variety of experiments [44,45]. Unfortunately, Er1221 seems to be on the other extreme from $ErRh_4B_4$, with the ferromagnetism actually being too weak to lead to the hoped for, exotic states that would emerge from the competition between the ferromagnetism and superconductivity. Despite several attempts to measure a spontaneous (zero field) flux line lattice it appears that such a state either does not exist, or is at best quite subtle. On the other hand the onset of this net ferromagnetic component does have dramatic effects on the vortex pinning, and therefore on the superconducting critical current.

6. Effects of magnetic order on vortex pinning and J_c

Another manifestation of how local moment magnetism interacts with superconductivity in the $R1221$ series can be seen manifesting itself in the degree of vortex pinning and therefore in the critical current, J_c. Vortex pinning is generally considered to be an extrinsic effect associated with chemical or structural defects in the sample (inclusions, doping, grain boundaries, etc.). As in the case of magnetic domain walls in industrial, hard ferromagnets, systematic control of pinning of vortices is key to the synthesis of useful superconducting wires, specifically for high current/high field applications. In the RNi_2B_2C series there are several intriguing examples of how the local moment order effects the vortex pinning. Perhaps the easiest example is associated with the weak ferromagnetic component that emerges in the Er1221 at lowest temperatures [46]. Fig. 11 plots the pinning strength as a function of temperature for Er1221. As can be seen below $T_{WF} \approx 2.3$ K the pinning strength increases dramatically. It has long been predicted that finely dispersed ferromagnetic impurities could act as pinning centers and enhance J_c [46], but one of the difficulties was to insure that the impurities would be small enough, homogeneously dispersed, and still retain their ferromagnetic properties without changing the basic superconducting properties of the host compound. Er1221 appears to solve these problems in an elegant manner: the ferromagnetism is not from impurities but instead from a long wave length ordering with a small ferromagnetic component.

Further investigation of Fig. 11 shows that even above T_{WF} the pinning strength has a well defined temperature dependence with a slope such that J_c appears to go to zero not at $T_c \sim 11$ K but instead at $T_N \sim 6$ K. Whereas J_c increasing dramatically at T_{WF} is not too difficult to understand, an increasing J_c associated with a purely antiferromagnetic order is a bit more curious. Detailed investigations show that below T_N, in the 0.55 a^* state, the sample experiences a magnetostriction that breaks the sample into a fine herring bone/tweed pattern of structural domains [47]. This very fine domain structure appears to be excellent for pinning vortices, in essence providing a plethora of grain

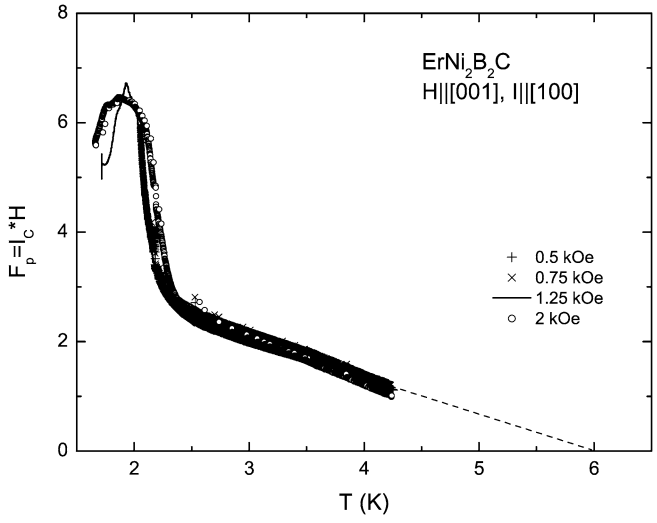

Fig. 11. Pinning force, $F_p \propto I_c H$, for $ErNi_2B_2C$. Dashed line is a guide for the eye. See [46] for a detailed discussion.

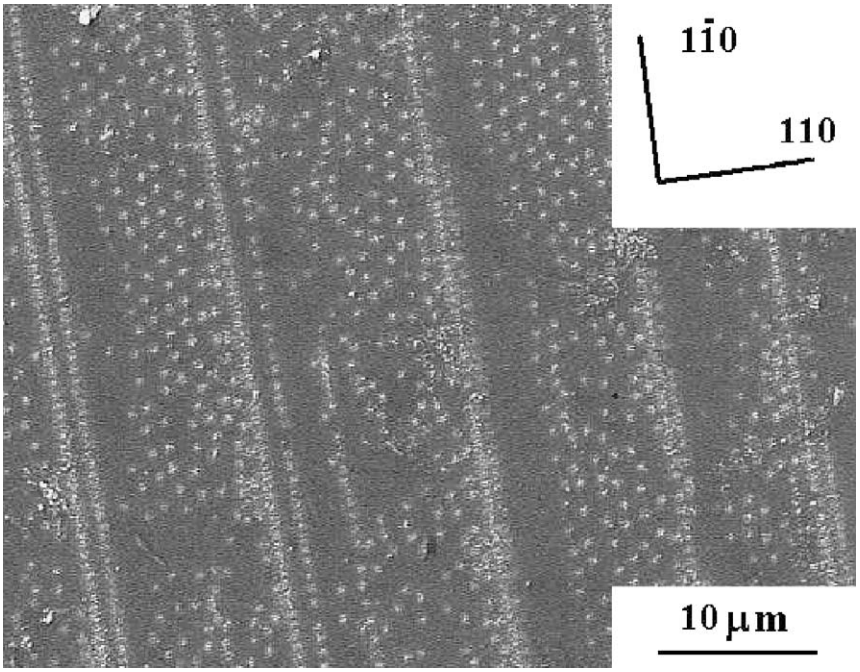

Fig. 12. Representative Bitter decoration pattern of vortices in $ErNi_2B_2C$. Magnetic field of 8 Oe is applied along the c-axis. The decoration temperature $T_d = 5.5\ \mathrm{K} < T_N$. Note high density of vortices on boundaries between domains. See [48] for further details.

boundary pinning (Fig. 12) [48]. A similar effect has been observed in Ho1221 over the very limited, but well defined, temperature and field range that Ho1221 is known to manifest a similar 0.55 a^* ordering [48,49].

7. Summary

In this review we have tried to present the range of effects that the magnetic ions of the rare earth series have on the superconductivity that is apparently ubiquitous to the heavier members of the RNi_2B_2C series. These effects can be arranged in a roughly hierarchal order. At the grossest level magnetism is detrimental to the superconducting ground state. In an Orwellian sense though, as far as superconductivity goes, all moments are detrimental; just some moments are more detrimental than others.

As the rare earth ion changes from the non-magnetic Y or Lu to magnetic Tm, Er, Ho, or Dy T_c is suppressed. On the other hand, there are mitigating circumstances. From dilution studies we can see that the suppression of T_c is proportionally larger for the more isotropic rare earths and less extreme for the extremely planar ones. The effects of this anisotropy can also be seen in $H_{c2}(T)$ curves with $H_{c2}(T)$ being more aggressively suppressed for the directions of applied field that give rise to the largest internal magnetizations. In addition, the state of magnetic sublattice is important. As one example, the superconductivity in $DyNi_2B_2C$ only exists because of the antiferromagnetic ordering of the Dy^{+3} sublattice. As another example, the superconductivity in $ErNi_2B_2C$ and $HoNi_2B_2C$ is suppressed in the vicinity of antiferromagnetic ordering that has a wave-vector associated with a Fermi-surface nesting feature.

The hierarchical cascade of effect that the rare earth will have on the superconducting ground state can then be summarized by a series of questions: (i) what is the rare earth; (ii) what is its anisotropy; and finally, (iii) what is the nature of the rare earth sublattice's long range order (or lack there of)?

In addition to the effects that the local moments have on T_c and $H_{c2}(T)$, there are equally clear effect on the pinning of vortices in the mixed state. Both $ErNi_2B_2C$ and $HoNi_2B_2C$ have a clear increase in the vortex pinning when the local moment order adopts the $\sim$0.55 a^* wave vector, leading, via magnetostriction, to a very fine grained state with clear pinning on the grain boundaries. Even more dramatic is the sharp increase of pinning associated with the onset of a small ferromagnetic component to the ordered state of Er1221 below $T_{\mathrm{wf}} \approx 2.3$ K.

In closing we should note that given the richness of phenomenon associated with the interaction between local moments and superconductivity it is not surprising that the RNi_2B_2C system has become one of the model systems

for studying this interplay. On the other hand, research on the $R\mathrm{Ni_2B_2C}$ system is far from over. Questions range from whether $\mathrm{ErNi_2B_2C}$ can be modified so as to allow for the unambiguous identification of a spontaneous flux line lattice, to whether the superconducting gap in any of the $R\mathrm{Ni_2B_2C}$ members manifests real nodes, or just deep minima? Given the ability to tune this series by substitution on both the R and Ni sites, and given the ability to grow large, high quality single crystals, the $R\mathrm{Ni_2B_2C}$ series will continue to provide insight to superconductivity and its interaction and response to local moment magnetism for years, and possibly decades to come.

Acknowledgements

We would like to thank the multitude of our collaborators who shared our excitement in studies of the rare earth–nickel–borocarbides. This work was written in anticipation of arrival of year 2005 Beaujolais Nouveau. Ames Laboratory is operated for the U.S. Department of Energy by Iowa State University under Contract No. W-7405-Eng.-82. This work was supported by the director for Energy Research, Office of Basic Energy Sciences.

References

[1] R.J. Cava, H. Takagi, H.W. Zandbergen, J.J. Krajewski, W.F. Peck Jr., T. Siegrist, B. Batlogg, R.B. van Dover, R.J. Felder, K. Mizuhashi, J.O. Lee, H. Eisaki, S. Uchida, Nature 367 (1994) 252.
[2] C. Mazumdar, R. Nagarajan, C. Godart, L.C. Gupta, M. Latroche, S.K. Dhar, C. Levy-Clement, B.D. Padalia, R. Vijayaraghavan, Solid State Comm. 87 (1993) 413.
[3] R. Nagarajan, C. Mazumdar, Z. Hossain, S.K. Dhar, K.V. Gopalakrisnan, L.C. Gupta, C. Godart, B.D. Padalia, R. Vijayaraghavan, Phys. Rev. Lett. 72 (1994) 274.
[4] B.K. Cho, P.C. Canfield, D.C. Johnston, Phys. Rev. B 52 (1995) R3844.
[5] R.J. Cava, H. Takagi, B. Batlogg, H.W. Zandbergen, J.J. Krajewski, W.F. Peck Jr., R.B. van Dover, R.J. Felder, T. Siegrist, K. Mizuhashi, J.O. Lee, H. Eisaki, S.A. Carter, S. Uchida, Nature 367 (1994) 146.
[6] P.C. Canfield, P.L. Gammel, D.J. Bishop, Phys. Today 51 (10) (1998) 40.
[7] K.-H. Müller, V.N. Narozhnyi, Rep. Progr. Phys. 64 (2001) 943.
[8] K.-H. Müller, G. Fuchs, S.-L. Drechsler, V.N. Narozhnyi, in: K.H.J. Buschow (Ed.), Handbook of Magnetic Materials, vol. 14, North-Holland, Amsterdam, 2002, p. 199.
[9] M.R. Eskildsen, P.L. Gammel, B.P. Barber, U. Yaron, A.P. Ramirez, D.A. Huse, D.J. Bishop, C. Bolle, C.M. Lieber, S. Oxx, S. Sridhar, N.H. Andersen, K. Mortensen, P.C. Canfield, Phys. Rev. Lett. 78 (1997) 1968.
[10] M. Yethiraj, D.M. Paul, C.V. Tomy, E.M. Forgan, Phys. Rev. Lett. 78 (1997) 4849.
[11] Y.D. Wilde, M. Yavarone, U. Welp, V. Metlushko, A.E. Koshelev, I. Aranson, G.W. Crabtree, P.C. Canfield, Phys. Rev. Lett. 78 (1997) 4273.
[12] L.Y. Vinnikov, T.L. Barkov, P.C. Canfield, S.L. Bud'ko, V.G. Kogan, Phys. Rev. B 64 (2001) 024504.
[13] M.R. Eskildsen, A.B. Abrahamsen, V.G. Kogan, P.L. Gammel, K. Mortensen, N.H. Andersen, P.C. Canfield, Phys. Rev. Lett. 86 (2001) 5148.
[14] P.L. Gammel, D.J. Bishop, M.R. Eskildsen, K. Mortensen, N.H. Andersen, I.R. Fisher, K.-O. Cheon, P.C. Canfield, V.G. Kogan, Phys. Rev. Lett. 82 (1999) 4082.
[15] K.-O. Cheon, I.R. Fisher, P.C. Canfield, V.G. Kogan, P. Miranovič, P.L. Gammel, Phys. Rev. B 58 (1998) 6463.
[16] V.G. Kogan, A. Gurevich, J.H. Cho, D.C. Johnston, M. Xu, J.R. Thompson, A. Martynovich, Phys. Rev. B 54 (1996) 12386.
[17] V.G. Kogan, M. Bullock, B. Harmon, P. Miranović, Lj. Dobrosavljević-Grujić, P.L. Gammel, D.J. Bishop, Phys. Rev. B 55 (1997) R8693.
[18] V.G. Kogan, P. Miranović, Lj. Dobrosavljević-Grujić, W.E. Pickett, D.K. Christen, Phys. Rev. Lett. 79 (1997) 741.
[19] Y. Maeno, T.M. Rice, M. Sigrist, Phys. Today 54 (1) (2001) 42.
[20] S.L. Bud'ko, P.C. Canfield, A. Yatskar, W.P. Beyermann, Physica B 230–232 (1997) 859.
[21] A. Yatskar, N.K. Budraa, W.P. Beyermann, P.C. Canfield, S.L. Bud'ko, Phys. Rev. B 54 (1996) R3772.
[22] S.K. Dhar, R. Nagarajan, Z. Hossain, E. Tominez, C. Godart, L.C. Gupta, R. Vijayaraghavan, Solid State Comm. 98 (1996) 985.
[23] E. Müller-Hartmann, J. Zittartz, Z. Phys. 234 (1970) 58.
[24] E. Müller-Hartmann, J. Zittartz, Solid State Comm. 11 (1972) 401.
[25] L.S. Borkowski, P.J. Hirschfeld, J. Low. Temp. Phys. 96 (1994) 185.
[26] M.D. Lan, T.J. Chang, C.S. Liaw, J. Phys. Chem. Solids 59 (1998) 1285.
[27] B.K. Cho, P.C. Canfield, D.C. Johnston, Phys. Rev. Lett. 77 (1996) 163.
[28] B.K. Cho, P.C. Canfield, L.L. Miller, D.C. Johnston, W.P. Beyermann, A. Yatskar, Phys. Rev. B 52 (1995) 3684.
[29] B.K. Cho, M. Xu, P.C. Canfield, L.L. Miller, D.C. Johnston, Phys. Rev. B 52 (1995) 3676.
[30] S.L. Bud'ko, V.G. Kogan, P.C. Canfield, Phys. Rev. B 64 (2001) 180506.
[31] A.I. Buzdin, L.N. Bulaevskii, M.L. Kulich, S.V. Panyukov, Usp. Fiz. Nauk 144 (1984) 597.
[32] L.N. Bulaevskii, A.I. Buzdin, M.L. Kulich, S.V. Panyukov, Adv. Phys. 34 (1985) 175.
[33] A.I. Buzdin, L.N. Bulaevskii, Usp. Fiz. Nauk 149 (1986) 45.
[34] S.L. Bud'ko, P.C. Canfield, Phys. Rev. B 61 (2000) R14932.
[35] K. Machida, K. Nokura, T. Matsubara, Phys. Rev. B 22 (1980) 2307.
[36] T.V. Ramakrishnan, C.M. Varma, Phys. Rev. B 24 (1981) 137.

[37] A.I. Goldman, C. Stassis, P.C. Canfield, J. Zarestky, P. Dervenagas, B.K. Cho, D.C. Johnston, B. Sternlieb, Phys. Rev. B 50 (1994) 9668.
[38] J.W. Lynn, S. Skanthakumar, Q. Huang, S.K. Sinha, Z. Hossain, L.C. Gupta, R. Nagarajan, C. Godart, Phys. Rev. B 55 (1997) 6584.
[39] K.D.D. Rathnayaka, D.G. Naugle, B.K. Cho, P.C. Canfield, Phys. Rev. B 53 (1996) 5688.
[40] W.A. Fertig, D.C. Johnston, L.E. DeLong, R.W. McCallum, M.B. Maple, B.T. Matthias, Phys. Rev. Lett. 38 (1977) 987.
[41] D.E. Moncton, D.B. McWhan, P.H. Schmidt, G. Shirane, W. Thomlison, M.B. Maple, H.B. MacKay, L.D. Wolf, Z. Fisk, D.C. Johnston, Phys. Rev. Lett. 45 (1980) 2060.
[42] S.K. Sinha, G.W. Crabtree, D.G. Hinks, H. Mook, Phys. Rev. Lett. 48 (1982) 950.
[43] P.C. Canfield, S.L. Bud'ko, B.K. Cho, Physica C 262 (1996) 249.
[44] S.-M. Choi, J.W. Lynn, D. Lopez, P.L. Gammel, P.C. Canfield, S.L. Bud'ko, Phys. Rev. Lett. 87 (2001) 107001.
[45] H. Kawano-Furukawa, H. Takeshita, M. Ochiai, T. Nagata, H. Yoshizawa, N. Furukawa, H. Takeya, K. Kadowaki, Phys. Rev. B 65 (2002) 180508.
[46] P.L. Gammel, B. Barber, D. Lopez, A.P. Ramirez, D.J. Bishop, S.L. Bud'ko, P.C. Canfield, Phys. Rev. Lett. 84 (2000) 2497.
[47] C. Detlefs, A.H.M.Z. Islam, T. Gu, A.I. Goldman, C. Stassis, P.C. Canfield, J.P. Hill, T. Vogt, Phys. Rev. B 56 (1997) 7843.
[48] L.Ya. Vinnikov, J. Anderegg, S.L. Bud'ko, P.C. Canfield, V.G. Kogan, Phys. Rev. B 71 (2005) 224513.
[49] C.D. Dewhurst, R.A. Doyle, E. Zeldov, D.M. Paul, Phys. Rev. Lett. 82 (1999) 827.